PUBLICATION IV

Modelling polymeric material using Microscale combustion calorimetry and other small scale data

Manuscript,
submitted to Fire and Materials
in June 2013.

MODELLING POLYMERIC MATERIAL USING MICROSCALE COMBUSTION CALORIMETRY AND OTHER SMALL SCALE DATA

Anna Matala and Simo Hostikka
VTT Technical Research Centre of Finland
P.O. Box 1000, FI-02044 VTT
anna.matala@vtt.fi

Keywords: pyrolysis modelling, Microscale combustion calorimetry, cables, PVC

Abstract

A challenge encountered by many practicing fire engineer carrying out fire modelling is that the combustible fuel is not completely well-known. Practical materials may, for instance, be identified as some well-known polymer, but this is usually not the whole truth from the viewpoint of the fire behaviour. Besides of the nominal polymer, the blend may include large quantities of different additives that affect the thermal degradation and combustion of the material. Until now, the effect of these additives has been taken into account in the modelling by adjusting the thermal parameters when fitting the model to the cone calorimeter results. Such a model captures the joint effect of all the components, but cannot distinguish between the combustible volatiles from additives and main polymer, which may lead to inaccurate prediction if the conditions, such as the heating rate, are significantly different. In this work we use Microscale Combustion Calorimetry for building a more accurate model of the polymer pyrolysis by combining the heat release rate measurements with the mass loss rate measured in Thermogravimetric Analysis. Two methods are developed and tested using a generic sample and a real PVC sheath of an electric cable. The results show that the methods are able to calculate the heat release rate correctly for the tested materials, and also estimating the sample composition to some extent.

Symbols

A	Pre-exponential factor (s^{-1})	*Greek*	
c_p	Specific heat capacity (kJ/kg/K)	α	Conversion
E	Activation energy (kJ/mol)	β	Heating rate (K/s)
ΔH	Heat of reaction (kJ/kg)	ε	Emissivity
ΔH_c	Heat of combustion (kJ/kg)	ρ	Density (kg/m^3)
k	Thermal conductivity (W/m/K)		
m	Mass (kg)	*Subscripts*	
$\dot{m}$	Mass loss rate (kg/s)	0	Initial
n_c	Number of components	eff	Effective value
n_{O2}	Reaction order of oxidation	F	Fuel gas
n_p	Number of (gaseous) products.	i	Reaction index
n_r	Number of reactions	I	Inert gas
N	Reaction order	j	Component index
Q_c	Heat release (kJ)	Z	Residue
$\dot{Q}_c$	Heat release rate (kW)		
Q/m_0	Total heat release in MCC (MJ/kg)		
Z	Residue yield (of total mass)		
T	Temperature (K)		

ΔT Temperature range
X_{O2} Oxygen volume fraction
y yield
Y Mass fraction

INTRODUCTION

Polymeric materials often include large amount of additives besides of the nominal polymer. The electrical cables, for instance, contain significant mass fractions of plasticizers, stabilizers and fillers. These additives are not reported by the manufacturer, and their concentrations are business secrets. This is a challenge commonly encountered by practicing fire engineer carrying out fire modelling. The problem is most pronounced in situations where the composition of the combustibles is not known at all, such as the fire investigation. The same problem is also faced when modelling industrial fires where the fuel may be formally known. The actual contents of the commercial material may be a very complicated blend of polymers and additives, as illustrated above for the electrical cables. A full chemical analysis of the combustible fuels could be used to reveal the contents of the fuels, at least qualitatively, but carrying out such an analysis would be impractical for many reasons. Simple and robust methods are therefore needed to determine the relevant pieces of information to support the fire modelling.

In this work, we use electrical cables as an example of material to be modelled. The additives of the cable components (e.g. phthalates, a plasticizer) are often combustible and may have other joint effects on the polymer degradation as well. In the pyrolysis modelling of the cable materials, these additives are usually taken into account simply by fitting the model to the experimental data [1]-[3]. The cone calorimeter has been until now the most commonly used experimental method that measures the heat release rate. The problem in cone calorimeter scale is that it only provides information about the effective heat of combustion, the joint effect of all the components degrading simultaneously. It does not provide information about the degradation temperatures or separate the heat release by reactions or components, which make the distinguishing between the components challenging.

Microscale Combustion Calorimetry (MCC) is a relatively new, experimental small scale device that was developed at Federal Aviation Administration (FAA) [4],[5]. It provides information about the heat release as a function of temperature, similarly to Thermogravimetric Analysis (TGA). By combining the information about mass loss and the simultaneous heat release, the heat of combustions of each reaction can be determined. Moreover, this information can be used in estimation of the sample composition and mass fractions.

In this work, the heat release rate measured by MCC is combined with mass loss measured by Thermogravimetric Analysis (TGA) at each reaction step. Two alternative methods are presented for building a reaction path using these results. The first one is a general model, which does not require any knowledge of the actual polymeric mixture. The second method is targeted for building a more complete and accurate model, and requires information about typical additives and their thermal degradation and heat of combustion. The results of both methods help to allocate the sample heat release to correct temperatures. Additionally, the second method can be used to estimate the mass fractions of main components in a polymer blend. These methods are applied to a generic sample in order to verify and validate the methods, and to a real PVC sheath of an electric cable. The results are compared in small and bench scale using experimental data and numerical simulations. The effect of surface oxidation is also taken into account in the cone calorimeter simulations.

METHODS

Experimental methods

TGA is the most common small scale experiment for determining the reaction kinetics of the pyrolysis reaction. In TGA, a small sample (5-10 mg) is placed into a furnace that has either air or nitrogen atmosphere. The furnace is heated linearly at relatively slow heating rate, typically at 1-30 K/min. The small sample and slow heating rate ensure that the sample is in thermal equilibrium with the furnace. The mass of the sample is measured during the heating, and the experiment results the mass loss as a function of temperature. [6]

MCC, also known as *Pyrolysis-combustion flow calorimetry*, was developed at FAA in the beginning of the millennium [4],[5]. A small sample (5-10 mg) is placed into a pyrolyzer that operates similarly to TGA under either inert of oxidative ambient. The heating rates are higher than typically in TGA experiment, usually 1 K/s. The pyrolysis gases are then led to a combustor that has high temperature (up to 1000 °C) and sufficient oxygen ambient. The gases are completely combusted in few seconds, and the result is the heat release rate (often scaled with the sample mass) as a function of temperature.

Cone Calorimeter is the most commonly used bench scale experiment in fire research. A 10 x 10 cm^2 sample is placed under a cone heater that directs a heat flux of 35-75 kW/m^2 to the sample surface. The sample is ignited using an electric spark. During the experiment, mass and heat release rates are measured. [7]

Combining TGA and MCC results

MCC measures the heat release rate scaled by the initial mass of the sample. For complete burning at heat of combustion ΔH_c and fuel yield $y_{i,F}$, the result can be expressed as

$$\frac{\dot{Q}_{c,i}}{m_0} = \frac{\dot{m}_{i,F}}{m_0}\Delta H_{c,i} = \frac{\dot{m}}{m_0} y_{i,F}\Delta H_{c,i}, \qquad (1)$$

where m_F corresponds to the mass loss that is responsible of the heat release (the production of the fuel gas). The total heat release of the reaction i (when temperature range of the reaction is T_{i-1} - T_i) can be written

$$\frac{Q_{c,i}}{m_0} = \int_{t_{i-1}}^{t_i} \frac{\dot{Q}_c}{m_0} dt = y_{i,F}\Delta H_{c,i} \int_{t_{i-1}}^{t_i} \frac{\dot{m}}{m_0} dt\,. \qquad (2)$$

The material is considered to be composed of j pseudo-components that each degrades in one or more reactions yielding potentially fuel gas (combustible), inert gas (e.g. water vapour) and residue. The yields of the products are denotes as y_{ijF}, y_{ijI} and y_{ijZ}, respectively. Naturally a component may yield several different fuel gases during one reaction, but in the accuracy of the model only the gross effect is significant. The total conversion ($\alpha = 1 - \frac{m}{m_0}$) of the reaction is

$$\Delta\alpha_i = \int_{t_{i-t}}^{t_i} \frac{\dot{m}}{m_0} dt = \frac{m_i - m_{i-1}}{m_0} = \sum_j (y_{ijF} + y_{ijI}) x_j, \qquad (3)$$

where x_i is the mass fraction of the component j. The overall fuel yield of the reaction is therefore

$$y_{iF} = \frac{Q_{c,i} / m_0}{\Delta H_{c,i} \Delta \alpha_i}. \qquad (4)$$

These results can be used in several ways, depending on the provided background information about the sample material. Therefore two methods were developed: *Method 1* is a general method for an unknown sample material. It does not require any information about the sample, just few assumptions by the user. *Method 2* targets to a more complete model with accurate information about the sample components. It makes assumptions about the reaction paths of the thermal degradation of the components and, in the best case, it can be used for determining the composition of the material.

Method 1 (blind approach)

For method 1, we assume that each reaction represents one pseudo-component, which release at most one fuel and one inert gas ($y_{i,F}+y_{i,I} = 1$ when $i<n_r$). Only the last reaction ($i = n_r$) yields also char. The reactions are well separated in time and each component degrades independently from the others. The modeller has to decide only two factors: The fuel gas (or the heat of combustion) and the inert gas (or the molar mass). These gases are assumed to be the same for all components and reactions. The reaction path of the Method 1 is shown in Figure 1.

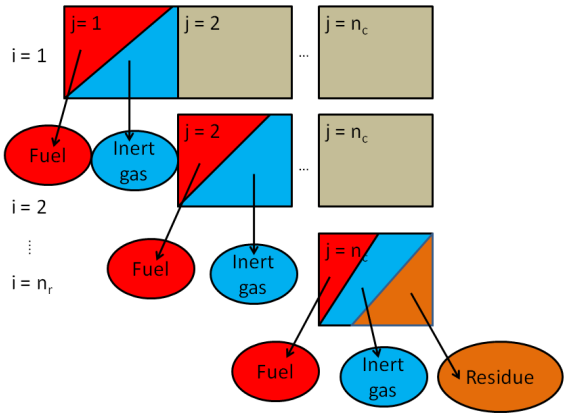

Figure 1. The reaction path assumption in Method 1.

The method is very straightforward: Since the mass loss of the reaction i ($i<n_r$) is equal to the mass fraction of the pseudo-component (x_i), eq. (4) can be used straight. For each reaction, an integral of the heat release rate, mass loss of the reaction and the constant heat of combustion are needed. For the last, residue yielding reaction the yields are calculated as

$$\begin{cases} y_{n_r F} = \dfrac{(Q_{c,n_r}/m_0)}{\Delta H_c \Delta\alpha_{n_r}}\left(1-\dfrac{Z}{1-\sum_{i=1}^{n_r-1}\Delta\alpha_i}\right) \\ y_{n_r I} = \left(1-\dfrac{(Q_{c,n_r}/m_0)}{\Delta H_c \Delta\alpha_{n_r}}\right)\left(1-\dfrac{Z}{1-\sum_{i=1}^{n_r-1}\Delta\alpha_i}\right) \\ y_{n_r Z} = 1-y_{n_r F}-y_{n_r I} = \dfrac{Z}{1-\sum_{i=1}^{n_r-1}\Delta\alpha_i} \end{cases}. \qquad (5)$$

Method 2 (advanced approach)

For method 2, an initial evaluation of the material composition has to be made. This method tries to follow the real reaction paths of the main components as accurately as possible while avoiding unnecessary complex model. The main components are those mainly responsible of the mass loss and heat release. Their typical reaction path and thermal degradation of the components can be studied from the literature. It assumed, that each component degrades in one or more reactions yielding several gases (both fuel and inert) and residue. The heat of combustion of inert gas is 0. Serial reaction paths are also possible, and several components may degrade simultaneously in the same reaction. A possible reaction path of the method 2 is shown in Figure 2.

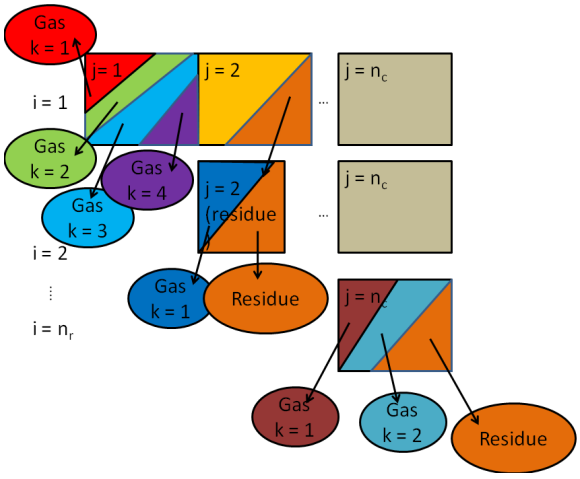

Figure 2. A possible reaction path in method 2.

The total heat release in each reaction *i* is estimated as

$$\hat{Q}_i = \sum_{j=1}^{n_c} \sum_{k=1}^{n_{p,j}} Y_{i-1,j} y_{i,j,k} \Delta H_{c,k} \ , \tag{6}$$

where $Y_{i,j}$ is the remaining mass fraction of the component j after reaction i. It is calculated from the initial mass fraction ($Y_{0,j}$) as

$$Y_{i,j} = \prod_{ii=1}^{i} y_{ii,j,Z} Y_{0,j} \ . \tag{7}$$

The estimate for the conversion (or mass loss) is

$$\Delta\hat{\alpha} = \sum_{j=1}^{n_c} \sum_{k=1}^{n_{p,j}} y_{i,j,k} Y_{i-1,j} \ . \tag{8}$$

The composition (initial mass fractions) can be solved by minimizing the error between the measured values and the calculated estimates as in

$$\min \sum_{i=1}^{n_r} \left(\frac{\left|\Delta a_i - \Delta\hat{a}_i\right|}{\Delta a_i} - \frac{\left| Q_i / m_0 - \hat{Q}_i \right|}{Q_i / m_0} \right). \tag{9}$$

This optimization problem can be solved e.g. using Matlab (function *fminsearch*) or Excel (solver). The solutions of the software depend strongly on the initial values. Therefore a Matlab script was generated to test several random initial values from the pre-defined range. The solution with smallest error is then selected as the final solution. The script is very fast to run; the time to perform 1000 iterations is few minutes.

The original mass fractions can also have some constrains according to the typical concentrations in similar applications. Sometimes the components or their products may react together resulting different reaction paths than the components individually. Also the reaction rate and other experimental circumstances are known to affect on gas and residue yields.

Numerical simulations

For verification and validation purposes, the TGA, MCC and cone calorimeter experiments were modelled using Fire Dynamics Simulator (FDS). All the numerical simulations are performed using FDS version 6.0 (release candidate 4, svn 15111) [8].

If the thermal equilibrium is maintained in TGA, it can be simulated using a 0-dimensional model. In order to make a 0-dimensional model of the sample with FDS, which is basically a 2 or 3-dimensional flow solver coupled with 1-dimensional pyrolysis model, the physical dimensions of the TGA were significantly altered to decouple the gas phase conditions from the sample response. In practice, the TGA sample modelled as a 0.1 mm thick slab with surface area of 2 m^2. The dimensions of the simulation domain were 4 m x 1 m x 1 m. All the gas phase reactions were prevented (nitrogen ambient), thus removing the dependence of the simulation on the gas phase cell size. The surrounding walls were heated linearly according to a slow, pre-determined heating rate from 20°C to 820°C. The thickness of the sample was small enough to keep it in thermal equilibrium with the environment. This was verified by measuring the temperatures of both the sample and the walls. The mass of the sample was monitored during the heating.

MCC experiment is identical to the TGA model in geometry, sample definition and omitting the gas phase calculation. The heat release rate is calculated as

$$\dot{q} = \dot{m}\Delta H_c . \qquad (10)$$

The heat release rate could be measured also directly by allowing gas phase calculation. However, then the grid cell size would be important parameter for the accuracy of the results, and the calculation would become significantly slower. The domain should also be divided to inert and oxidative ambient, which would increase the domain size even further. Therefore, this simplistic method for MCC experiment is chosen.

When the simulated TGA and MCC results are compared, it can be observed that in FDS the high heating rates move the reaction to higher temperatures. This behaviour can be observed in the experiments as well, but not nearly as much. The sample is in thermal equilibrium with the furnace, as can be observed in Figure 3 a. However, the increasing the heating rate of a simulation from 10 K/min to 60 K/min moves the curve about 50 K to higher temperatures (Figure 3b). This can be explained with the kinetic parameters. Sometimes, the reaction is slow compared to the heating rate. Although the reaction rate of the thermal degradation reaction is independent on the reaction rate, the temperature of the sample increases faster than the reaction can occur. Therefore at high heating rates it seems like the reaction has moved to higher temperatures.

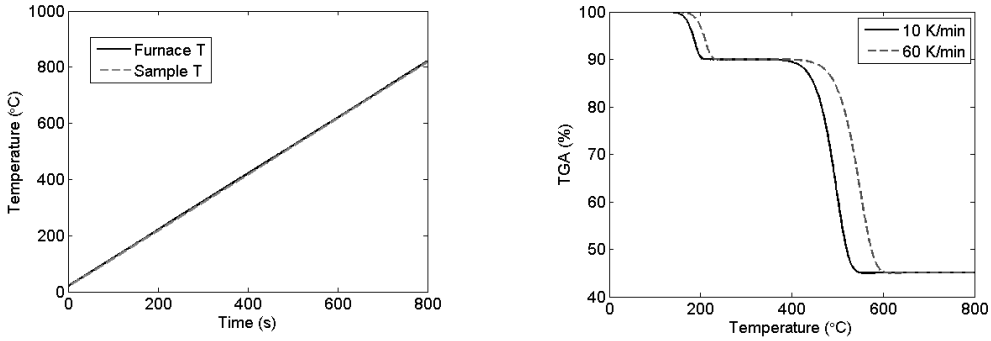

Figure 3. Results of TGA/MCC simulation. a) Comparison of furnace and sample temperature at 60 K/min. b) TGA at 10 and 60 K/min.

In cone calorimeter experiments usually the cable is tested as whole, not divided into components as in the small scale experiments. The cables and all other complex structures are modelled as rectangular slabs. That works relatively well in coarse applications, but the solution is always limited by the grid size. Also the geometry is strongly simplified when the cylindrical object consisting of multiple components is treated as a laminate of separate, rectangular layers. This model has a domain of 0.3x0.3x0.4 m^3 and grid size of 5 cm. The grid size is quite coarse but it should be similar to the one in the final application. The cone heater is modelled as an external heat flux (50 kW/m^2) directed to the surface of the sample. The structure of the layers is symmetric.

MATERIALS

Generic materials

Three generic materials are developed. These samples represent ideal samples, where all reaction steps are well-defined and known. They do not correspond to any real material, and the parameters are listed only for completeness. Generic sample 1 is used to verify the calculations and simulation methods in a very simple case. The Generic sample 2 is made for verification with a more complex case where the first reaction has a small mass loss with high heat of combustion, and the second

reaction high mass loss with low heat of combustion. The accuracy of the reaction path for a PVC-like material is assessed with Generic sample 3. Other than kinetic parameters are same for all the samples and components, including char ($\varepsilon = 1.0$, $c_p = 1.0$ kJ/kg·K, $k = 1.0$ W/m·K, $\rho_0 = 100$ kg/m^3, $\Delta H = 0$ kJ/kg).

Generic 1 is the simplest test case with only one reaction step. It yields 0.9 of the mass fuel gas with heat of combustion 35 MJ/kg. The parameters are listed in Table 1 .

The second test case, Generic 2, yields little mass and lots of energy at the first reaction step, and the second releases lots of mass and little energy. The reaction parameters are listed in Table 1 and visually shown in Figure 4a.

For testing the method for more complex sample, a third generic material (Generic 3) is used. The kinetics or other parameters do not represent any specific material, and the kinetic parameters of components 1 and 3 are identical to those of Generic 2. The reaction path resembles the one of plasticized PVC. It has two initial components (Comp 1 and Comp 2) as the PVC polymer and the plasticizer. They start to thermally degrade in close to the same temperatures. The earlier reaction yields some fuel gas, inert gas (as Hydrocloric acid (HCl) in PVC) and residual polymer that degrades further in higher temperatures. The second initial component releases fuel gas and no residue during the first reaction step. All the parameters are listed in Table 1 and the simulated results are shown in Figure 4b.

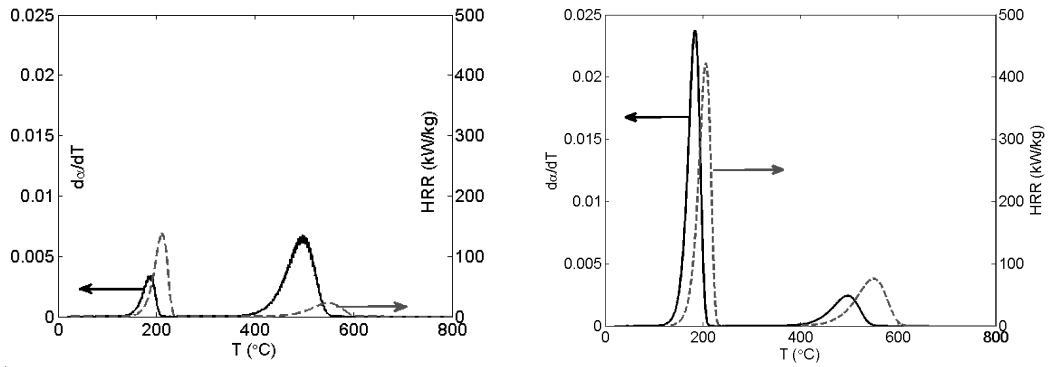

Figure 4. Generic samples. TGA results are shown on the left axes and MCC results on the right. a) Generic 2 sample. b) Generic 3 sample.

Table 1. Reaction parameters and resulting mass loss and energy release of each reaction for the generic samples 1, 2 and 3.

	Generic 1	*Generic 2*		*Generic 3*		
	Comp 1	*Comp 1*	*Comp 2*	*Comp 1*	*Comp 2*	*Comp 3*
Mass fraction in virgin material	1.0	0.5	0.5	0.7	0.3	0.0
A (s^{-1})	$1.0 \cdot 10^{10}$	$1.0 \cdot 10^{15}$	$1.0 \cdot 10^{10}$	$1.0 \cdot 10^{15}$	$1.0 \cdot 10^{16}$	$1.0 \cdot 10^{10}$
E (J/mol)	$1.6 \cdot 10^{5}$	$1.48 \cdot 10^{5}$	$1.8 \cdot 10^{5}$	$1.48 \cdot 10^{5}$	$1.55 \cdot 10^{5}$	$1.8 \cdot 10^{5}$
gas yield	0.9 (fuel)	0.2 (fuel)	0.1 (fuel) 0.8 (inert)	0.02 (fuel) 0.58 (inert)	1.0 (fuel)	0.6 (fuel)
ΔHc (MJ/kg)	35	45	35	30	35	42
Residue?	Char	Char	Char	Comp 3	No residue	Char
Peak Temperature (°C) at 10 K/min	420	180	500	180	180	500
Δα	0.9	0.1	0.45	0.72		0.17

Q/m_0	31.5	4.5	1.75	13.02	5.88

PVC sheath

Real plasticized PVC can be significantly more complex than the generic example presented above. Therefore the methods are applied to a real thermoplastic cable with PVC sheath and PE insulation. The cable is the number #701 in the Christifire campaign (GENERAL CABLE® BICC® BRAND SUBSTATION CONTROL CABLE 7/C #12AWG 600V 30 MAY 2006). It has 7 conductor and diameter of 14 mm. All the other details can be found from the ref. [9]. The experimental data set included TGA results at 10 K/min and three repeated MCC results at 60 K/min for sheath and insulation. The experimental small scale results are listed in Table 2. In addition, cone calorimeter results at 25 KW/m^2, 50 KW/m^2 and 75 KW/m^2 were available. The experimental results for the PVC sheath are shown in Figure 5. An average of the three repetitions of the MCC experiment was used.

Table 2. Experimental results for PVC sheath and PE insulation of cable #701.

	Sheath			Insulation		
	Reac 1	Reac 2	Reac 3	Reac 1	Reac 2	Reac 3
$\Delta\alpha$	0.600	0.137	0.040	0.570	0.120	0.052
Q/m_0 (MJ/kg)	9.195	4.905	0.000	8.233	4.770	0.000

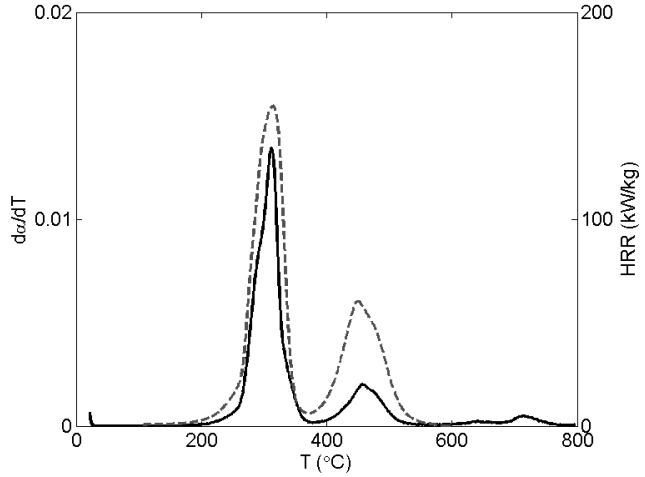

Figure 5. Experimental TGA (10 K/min) and MCC (60 K/min) results for PVC sheath. The experimental results are slightly filtered.

Understanding the basics of PVC blend degradation is important if more accurate reaction path is required. The theoretical background of the degradation of PVC and the most significant additives is therefore briefly presented here.

The thermal degradation of pure and plasticized PVC has been studied widely in the literature, experimentally ([10]-[16]) and numerically ([15]-[21]). Overall, the thermal degradation of the PVC is a two stage process. The first reaction around 320 °C is often called dehydrochlorination reaction, because it is mainly responsible of release of HCl. The remaining polyene structure starts degrading immediately releasing small amounts of aromatic hydrocarbons, mainly benzene. The second major reaction occurs around 450 °C, and is the pyrolysis of the polyene residue. The main product of this reaction is toluene. [10],[12],[17] Studied in vacuum [16], the mass loss of the first reaction was 64

%, which is higher than the stoichiometric value 58.7 %. Therefore the amount of benzene release in the first reaction was 5.3%. The mass loss of the second reaction was 30.3 % leaving 5.7 % residue.

Various additives have effect on the thermal degradation of PVC. The most important additive in many PVC applications (including cables) is the plasticizer. The concentrations can be as high as 100 phr (parts per hundred parts of resin). There are several commercial plasticizers available, and one of the most commonly studied of them is Di-2-ethylhexyl phthalate (DOP). Marcilla and Beltrán compared pure samples of DOP and PVC resin to mixtures at different concentrations and heating rates [15]. The plasticizer degrades around the same temperatures as the dehydrochlorination reaction, but carefully looking two peaks can be observed; DOP evaporates slightly before HCl. When the peak temperatures are compared, it can be seen that in mixture the reactions are closer to each other, almost overlapping: DOP evaporates slightly later, and HCl slightly earlier than separately. Low concentrations of DOP decrease this effect. Also, at higher heating rates the decrease in resin degradation temperature is not as significant as at the lower heating rates. One explanation for the decreasing HCl release temperature is that when the DOP evaporates, it leaves holes to the polymer blend structure. These holes are the initiation centres of the dehydrochlorination process and the reaction becomes faster. Another explanation is that the radicals formed around 300 °C at the DOP evaporation promote the reaction. DOP is also known to partially inhibit the release of the aromatics formation. [12],[13],[15]

PVC blend also includes some amount of fillers. Calcium Carbonate ($CaCO_3$) is the most commonly used with PVC. It is used to improve the impact resistance and thermal stability. Typical concentrations are 20-30 wt% in rigid and 30-40 wt% in flexible PVC. [22] It may react with HCl producing calcium chloride. It also degrades at high temperatures (above 840 °C) producing CO_2 and H_2O.

Other significant additives are stabilizers and metal oxides, although their concentrations are not very high. The stabilizers do not affect on the degradation temperatures, but they seem to inhibit the formation of the HCl. In higher concentrations (> 1 phr) they also seem to inhibit the formation of benzene and toluene [13]. Metal oxides suppress the amount of released aromatic hydrocarbons. Some oxides also lower the temperature of the dehydrochlorination reaction. Those metal oxides that suppress most benzene formation also promote char under nitrogen ambient. [10] The role of these additives is not investigated in this paper.

The insulation layer is nominally a polyethylene (PE) blend. Pure PE degrades around 400-500 °C without leaving residue. The additives are assumed to be similar to those of PVC for simplicity. [23]

RESULTS

Generic samples

The calculation and simulation methods were first verified by using the Generic 1 sample. The results show that the correct amount of heat can be allocated to each reaction using both methods. Additionally, it showed that the FDS model indeed calculates the mass and heat release as expected.

The Generic 2 sample undergoes two reactions. Both of them yield fuel and residue, the second also inert gas. The experimental results and the target values were listed in Table 1. These results are confirmed by integrating over the reaction steps of the FDS results. The mass fractions of the components are assumed known (0.5 for both components), and the other parameters are listed in

Table 3. For both methods the reaction specific mass loss and heat release are calculated correctly with these parameters. Method 2 only slightly (3 %) overestimates the mass loss of the reaction 2 (0.46), but the total heat release is exactly 1.75 MJ/kg.

Table 3. Estimation results and estimation boundaries for method 2 of sample Generic 2.

	y_{I11}	y_{F11}	y_{I22}	y_{F22}	$\Delta H_{c,11}$ (MJ/kg)	$\Delta H_{c,22}$ (MJ/kg)
Exact value	0.00	0.20	0.80	0.10	45.00	35.00
Method 1	0.03	0.97	0.46	0.04	46.45	46.45
Method 2	0.01	0.19	0.81	0.12	47.02	30.07
Est. boundaries	[0,1]	[0,0.3]	[0,1]	[0,0.3]	[30, 50]	[30, 50]

The Generic 3 sample undergoes three fuel yielding reactions. Two first reactions (Comp 1 and Comp 2) are overlapping and inseparable in time or temperature. The net energy release in the first reaction should be (according to Table 1) 13.02 MJ/kg and in the second 5.88 MJ/kg, making the total heat release of the sample 18.90 MJ/kg. The corresponding mass losses should be 0.72 and 0.17. An integral over the peaks confirm these results.

For **Method 1**, we assume that the heat of combustion of the fuel gas is 40 MJ/kg. For the first reaction, the parameters are $Q_{c,1}/m_0$ = 13.02 MJ/kg, $\Delta\alpha_1$ = 0.72 and ΔH_c = 40 MJ/kg. According to eq. (4), the fuel yield (y_{1F}) is 0.45 (and the yield of the inert gas is therefore 0.55). For the second reaction, we have to take the char yield into account. The total char yield of the material (Z) is 0.11. The fraction of the fuel of all the gas released in the second reaction is by eq. (4) 0.865. The yields are then calculated as in eq. (5)

$$\begin{cases} y_{2F} = 0.865\left(1-\dfrac{0.11}{1-0.72}\right) = 0.53 \\ y_{2I} = (1-0.865)\left(1-\dfrac{0.11}{1-0.72}\right) = 0.08 \\ y_{2Z} = 1-0.53-0.08 = 0.39 \end{cases}.$$

The results are summarized in Table 4.

Table 4. The yields and mass fractions for generic sample 3 using Method 1.

	y_F	y_I	y_Z	Y
Reaction 1	0.45	0.55	0.0	0.72
Reaction 2	0.53	0.08	0.39	0.28

For **method 2** we assume that the material is a PVC polymer with some plasticizer. We set the estimation boundaries as listed in Table 5. The estimation problem was solved using a Matlab function and a script that tried random initial values and chose the values that gave the smallest error. The iteration with random initial values was performed 5000 times, and the best solution gave an error of $5.8 \cdot 10^{-8}$. The values for the final estimation results can be seen in Table 5. The results are relatively near the target values considering the width of the estimation boundaries.

Table 5. Estimation boundaries, initial values and the final results for the Generic 3 sample. The first subscript denotes to reaction and second to component (PVC = 1, plasticizer = 2).

Variable	Boundaries	Initial value used	Target value	Estimation result	Error
Y_1 ("PVC")	[0.5, 0.8]	0.59	0.70	0.70	0 %
Y_2 ("Plasticizer")	-	0.41	0.30	0.30	0 %
y_{I11}	[0.57, 0.61]	0.58	0.58	0.60	-3 %
y_{F11}	[0, 0.05]	0.00	0.02	0.00	100 %
y_{F12}	[0.5, 0.9]	0.67	0.60	0.61	-2 %
ΔH_{c11} (MJ/kg)	[20, 45]	30.27	30.0	27.60	8 %
ΔH_{c12} (MJ/kg)	[20, 45]	34.28	35.0	34.59	1 %
ΔH_{c21} (MJ/kg)	[20, 45]	36.05	42.0	43.04	-2 %

The results with Method 1 and Method 2 were next tested by investigating if the resulting parameters can reproduce the mass loss and heat release characteristics of the generic data. This was done by calculating the TGA and MCC experiments using both reaction paths. The kinetic parameters are assumed to be known exactly (for Method 1, only those of the Comp 1 are used for the first reaction). The results confirm that although the reaction paths and assumptions are different, the essential information (mass loss and heat release) can be repeated correctly using both methods. The results are shown in Figure 6.

In addition to the mass and energy calculation, the capability of method 2 was validated by comparing the estimated and target values. The errors between these two values are listed in Table 5. In general, the estimated values are within 10 % to the real ones. However, the greatest error is with the fuel yield of the Comp 1 in reaction 1. As the amount of fuel from the PVC is very small, this error is irrelevant.

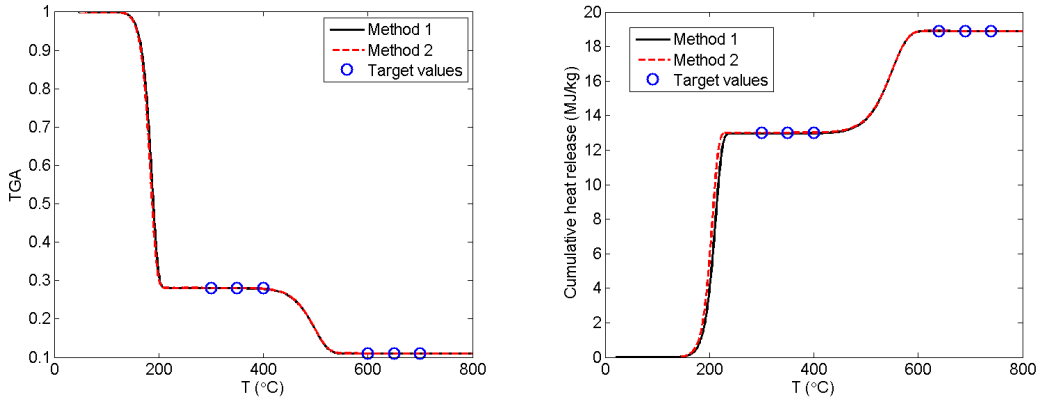

a) b)

Figure 6. Verification of the estimation results. a) Mass loss (TGA at 10 K/min in N_2). b) Energy release (MCC at 60 K/min in air).

Application to a real PVC sheath

Small scale model

As seen in Figure 5, the TGA results show three reaction peaks, MCC results only two. As listed in Table 2, the measured heat releases are 9.195 MJ/kg in the first reaction and 4.905 MJ/kg in the second. The mass losses are 0.6, 0.137 and 0.04, correspondingly. The kinetic parameters (A, E, N) were estimated using Genetic Algorithm (GA) ([2],[9]) for both methods (different reaction paths) separately. The kinetic parameters are known to compensate the other parameter values so that there may be several sets of equally fitting parameters. To minimize this effect, the parameters should be estimated at several heating rates. Unfortunately, the experimental data set only included on heating rate at 10 K/min. However, from the MCC results (at 60 K/min) it can be seen, that the reactions happen almost simultaneously as seen in Figure 5. Therefore the parameters are estimated at these two heating rates, using the same experimental results from 10 K/min.

The reaction path parameters were estimated similarly for the insulating material that was known to be PE. It had similarly three mass loss peaks, the third one without heat release. The mass losses of the reactions were 0.57, 0.12 and 0.052. The heat releases of the two first reactions were 8.233 MJ/kg and 4.77 MJ/kg.

Method 1: The fuel in this model was assumed to be propane (46.45 MJ/kg) and the inert gas water vapour. The fuel yields are calculated according eq. (4) and eq. (5) and the results are listed in Table 6. The reaction path and the kinetic parameters are shown in Figure 7. The comparison between experimental and simulated small scale results are seen in Figure 9.

With similar assumptions of the fuel gas as for the sheath material, the fuel yields of the insulation material are 0.31 and 0.86 in two first reactions. The third reaction does not yield fuel gas, and residue yield is 0.83. The kinetic parameters are listed in Table 8.

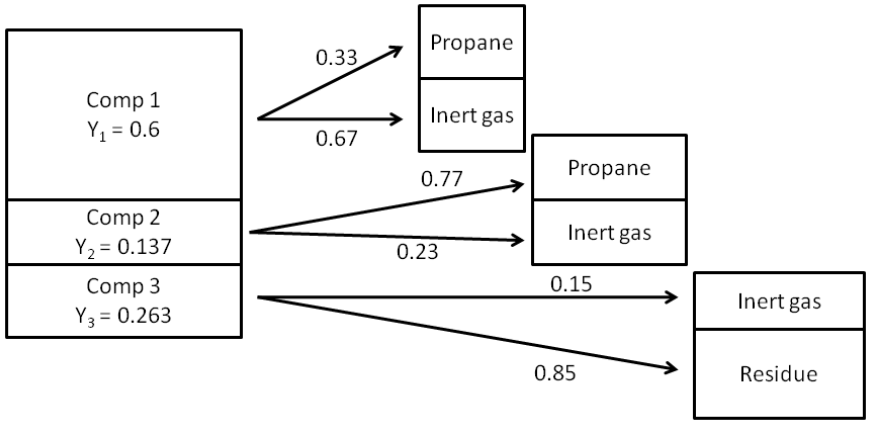

Figure 7. Reaction path and kinetic parameters for the PVC sheath using Method 1.

Table 6. Estimation results for PVC sheath and PE insulation using Method 1.

	Reaction i	Y_i	y_{Fi}	y_{Ii}	y_{Ri}
Sheath (PVC)	1	0.600	0.33	0.67	0.00
	2	0.137	0.77	0.23	0.00
	3	0.263	0.00	0.15	0.85
Insulation (PE)	1	0.57	0.31	0.69	0.00
	2	0.12	0.86	0.14	0.00
	3	0.31	0.00	0.17	0.83

Method 2: The reaction path of the real PVC sheath was assumed similar to the Generic 2 sample, and the third additional reaction (with no measured heat release) was assumed to be due to $CaCO_3$ thermal degradation. The estimation boundaries are listed in Table 7. The optimization was performed using the Matlab script mentioned before. In 5000 iterations, the minimum was found with error (eq. (9)) of $2.4 \cdot 10^{-7}$. The resulting values are listed in Table 7 and the reaction path and kinetic parameters are shown in Figure 8. The comparison between experimental and simulated small scale results are shown in Figure 9.

The insulating material was known to be PE. Pure PE is thermoplastic and therefore does not yield residue. The first reaction corresponds to the temperature range of the plasticizer, and second to the degradation of the PE. The third reaction is again assumed to be due to $CaCO_3$. As the two fuel yielding components do not yield any char (at least, not in their pure form), the mass losses of the reactions are used as the mass fractions of the components. The calculation of the heat of combustions is very straight-forward and they can be calculated using eq. (4). As result, the heats of combustions for two first reactions are 14.45 MJ/kg and 39.73 MJ/kg, respectively. The residue yield of the last reaction is 0.83.

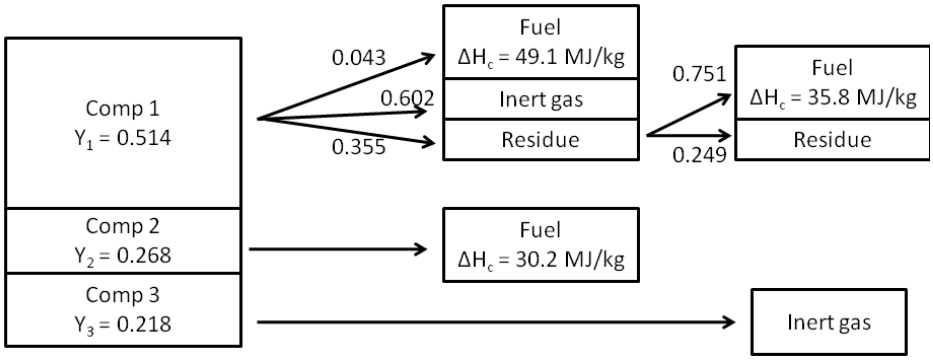

Figure 8. Reaction path and kinetic parameters for a PVC sheath using Method 2.

Table 7. Estimation boundaries, initial values and the final estimated values of the PVC sheath using Method 2.

	Estimation boundaries	Initial values	Estimation result
Y_1	[0.2, 0.7]	0.508	0.514
Y_2	[0.1, 0.5]	0.323	0.268
Y_3	-	0.169	0.218
y_{I11}	[0.57,0.61]	0.606	0.602
y_{F11}	[0, 0.07]	0.040	0.043
y_{F12}	[0.5, 0.9]	0.786	0.751
y_{I13}	[0.05, 0.3]	0.186	0.184
ΔH_{c11} (MJ/kg)	[25, 50]	48.9	49.1
ΔH_{c12} (MJ/kg)	[25, 50]	31.2	35.8
ΔH_{c21} (MJ/kg)	[25, 50]	32.1	30.2

Table 8. The kinetic parameters for PVC sheath and insulation using Method 1 and Method 2.

Material	Method	Component (i) Reaction (j)	A (s^{-1})	E (mol/kJ)	N
Sheath (PVC)	Method 1	i = j= 1	$3.6 \cdot 10^{21}$	$2.4 \cdot 10^{5}$	2.87
		i = j = 2	$1.2 \cdot 10^{29}$	$3.8 \cdot 10^{5}$	4.10
		i = j = 3	$5.1 \cdot 10^{21}$	$3.0 \cdot 10^{5}$	2.67
	Method 2	i = 1,2, j = 1	$2.1 \cdot 10^{26}$	$2.8 \cdot 10^{5}$	3.69
		i = 1, j = 2	$2.0 \cdot 10^{25}$	$3.2 \cdot 10^{5}$	4.91
		i = 3, j = 3	$9.8 \cdot 10^{24}$	$2.9 \cdot 10^{5}$	0.96
Insulation (PE)	Both methods	i = j = 1	$1.26 \cdot 10^{25}$	$2.7 \cdot 10^{5}$	3.20
		i = j = 2	$1.9 \cdot 10^{27}$	$3.6 \cdot 10^{5}$	3.7
		i = j =3	$1.6 \cdot 10^{12}$	$2.1 \cdot 10^{5}$	4.41

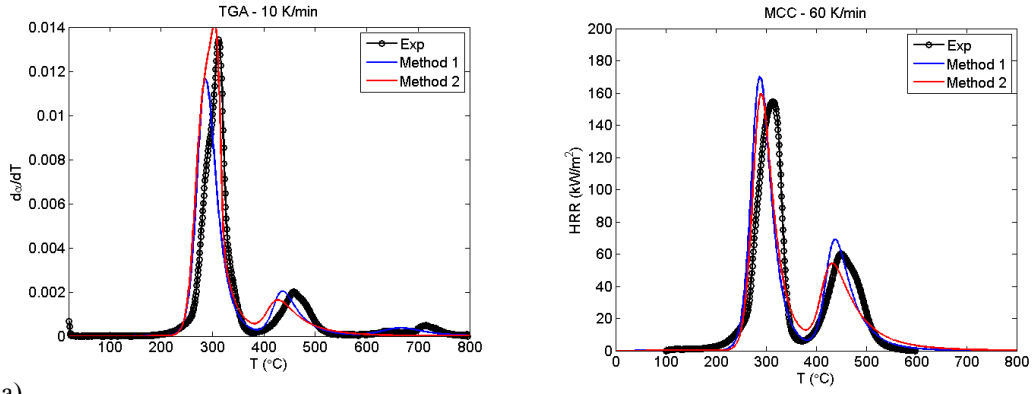

a) b)

Figure 9. Comparison of the experimental and simulated results for real PVC sheath. a) TGA. b) MCC.

Bench scale model

The cone calorimeter experiments were performed at 25, 50 and 75 kW/m^2 heat fluxes. The experimental results are listed at Table 9. The mass fractions of the components were 0.24 (sheath), 0.18 (insulation) and 0.58 (conductor). Conductor is non-combustible. The total mass loss of the sheath is 77.7 % and of insulation 74.2 % and total heat release 14.1 MJ/kg and 13.0 MJ/kg,

respectively. Multiplying by mass fractions and the initial mass 270 g, the mass loss is 84.8 g (32 %) and the total heat release 1.52 MJ. The effective heat of combustion (total heat release scaled by the mass loss) is then 17.9 MJ/kg. This is less than in cone calorimeter experiments at 25 and 50 kW/m^2. The extra heat released is related to the oxidation of char. This phenomenon is addressed in the next section.

Table 9. Experimental cone calorimeter results.

	25 kW/m^2	50 kW/m^2	75 kW/m^2
m_0 (g)	263.9	269.0	262.2
Δm (g)	71.0	91.2	89.0
$\Delta m/m_0$ (g/g)	0.27	0.34	0.34
Q_{tot} (MJ)	1.92	1.71	1.59
$\Delta H_{c,\,eff}$ (MJ/kg)	27	18.75	17.9

The cone calorimeter models were developed based on the small scale results and mass fractions. The results are listed in Table 10 and graphically presented in Figure 10. The cone calorimeter models where calculated using FDS 6 with 5 cm grid resolution. The parameters were fitted at 50 kW/m^2 heat flux, and validated using results of 25 and 75 kW/m^2 heat fluxes.

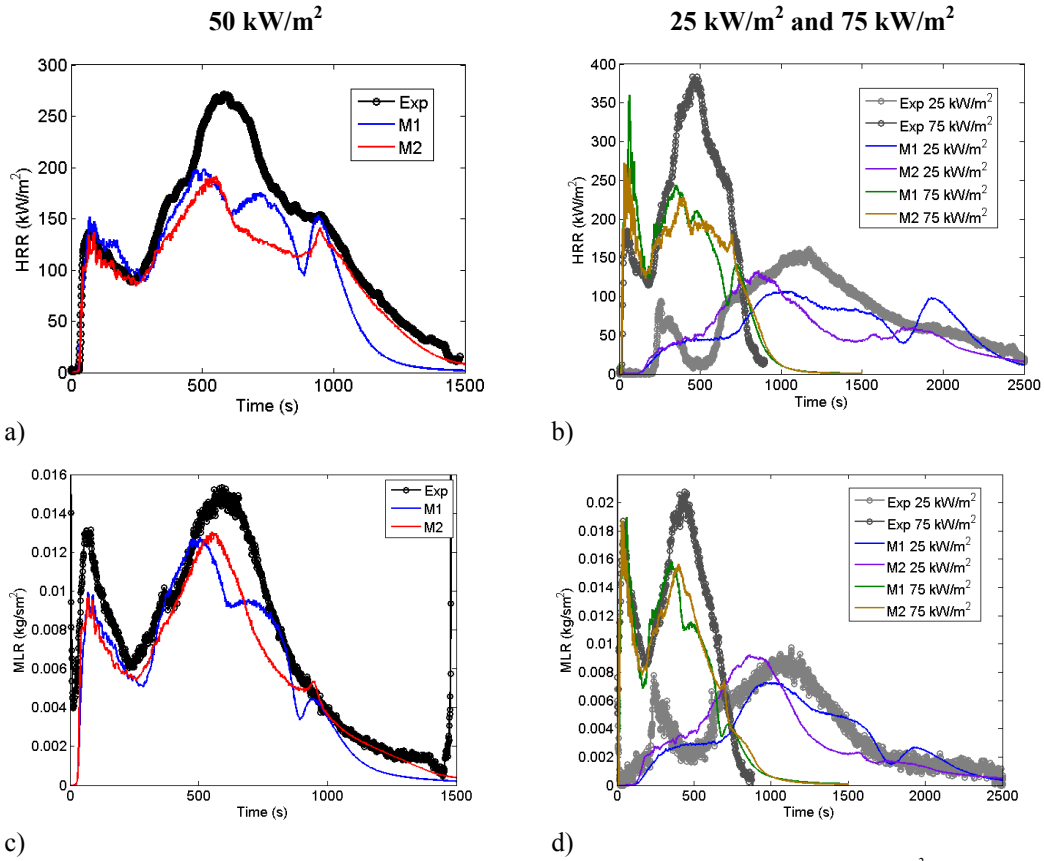

Figure 10. Cone calorimeter results for Method 1 and Method 2. a) Heat release rate at 50 kW/m^2. b) Heat release rate at other heat fluxes. c) Mass loss rate at 50 kW/m^2. d) Mass loss rate at other heat fluxes.

Table 10. Thermal parameters of cable 701.

			Method 1	Method 2		
				Polymer	Plasticizer	$CaCO_3$
Sheath	Reaction 1	k (W/(mK))	0.147	0.146	0.185	0.48
		c_p (kJ/(kgK))	3.22	3.4	2.8	3.5
		ΔH (kJ/kg)	1607	206	1112	1669
		ε	0.7	1.0	1.0	1.0
	Reaction 2	k (W/(mK))	0.175	0.2	-	-
		c_p (kJ/(kgK))	3.45	2.26	-	-
		ΔH (kJ/kg)	1425	1783	-	-
		ε	1.0	1.0	-	-
	Reaction 3	k (W/(mK))	0.103	-	-	-
		c_p (kJ/(kgK))	3.5	-	-	-
		ΔH (kJ/kg)	43	-	-	-
		ε	1.0	-	-	-
	Residue	ρ (kg/m^3)	344	70		274
		k (W/(mK))	0.122	0.188	-	0.188
		c_p (kJ/(kgK))	3.5	2.0	-	2.0
		ε	0.85	1.0	-	1.0
Insulation	Reaction 1	k (W/(mK))	0.783	0.246	-	-
		c_p (kJ/(kgK))	3.36	1.9	-	-
		ΔH (kJ/kg)	1408	1760	-	-
		ε	1.0	1.0	-	-
	Reaction 2	k (W/(mK))	1.0	-	0.59	-
		c_p (kJ/(kgK))	3.4	-	3.0	-
		ΔH (kJ/kg)	1516	-	691	-
		ε	1.0	-	1.0	-
	Reaction 3	k (W/(mK))	0.087	-	-	0.285
		c_p (kJ/(kgK))	2.74	-	-	2.9
		ΔH (kJ/kg)	445	-	-	353
		ε	1.0	-	-	1.0
	Residue		297	-	-	297
		k (W/(mK))	0.01	-	-	0.338
		c_p (kJ/(kgK))	1.29	-	-	1.29
		ε	1.0	-	-	1.0

Surface oxidation

It was noticed that the heat release and mass loss in cone calorimeter was higher than according to small scale results should be. This was speculated to be due to surface oxidation, and this can be confirmed by comparing TGA results in air and nitrogen. In air the mass loss of the sheath is 7.7% higher than in nitrogen. This corresponds to 1.7 % (4.6 g) mass loss in the whole cable. The heat released in cone calorimeter is about 0.17 MJ more than that of the models. Dividing the heat by the mass loss gives heat of oxidation about 37 MJ/kg.

The newest version of FDS 6 is currently able to model the oxidation as function of available oxygen [8]. The reaction rate defined by Arrhenius parameters is multiplied by a function of oxygen volume fraction of the first gas cell

$$r_{ij} = A_{ij}\left(\frac{\rho_i}{\rho_0}\right)^{n_{ij}} \exp\left(-\frac{E_{ij}}{RT}\right) X_{O_2}^{n_{O_2,ij}} . \qquad (11)$$

In normal pyrolysis reaction order of oxidation is 0. Deeper under the surface the oxygen concentration depends on the diffusion depth, also defined by user. The parameters are found by comparing the model with the last reaction of TGA experiment in air. For method 1, the oxidation reaction is one parallel reaction more. For method 2, the char yielded by PVC and $CaCO_3$ is converted into ash. The parameters of this reaction are listed in Table 10 and visually shown in Figure 11. The pyrolysis reactions do not fit exactly to the experimental data. Part of the reason may be the ignition model of FDS. In FDS, whenever oxygen is present, the fuel gas ignites. In real TGA this hardly happens, since the temperatures of most degradation steps are below the autoignition temperature. However, also in the experiment the fuel reacts with oxygen in some level, releasing heat. For these reasons, the only significant part of the curve is in the end, corresponding to the surface oxidation.

The cone calorimeter results are shown in Figure 12. It seems that the oxidation alone does not explain the different mass loss and heat release results in the cone calorimeter.

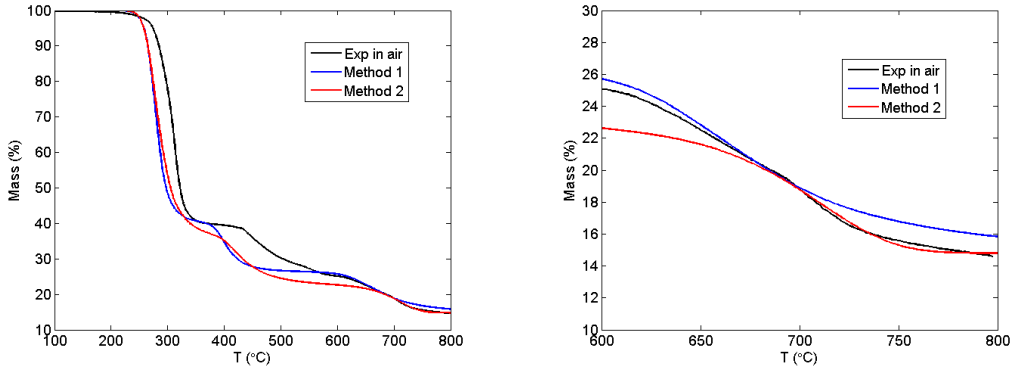

Figure 11. Implementing the oxidation reaction. a) TGA in air. b) Zoomed in to the end of the experiment.

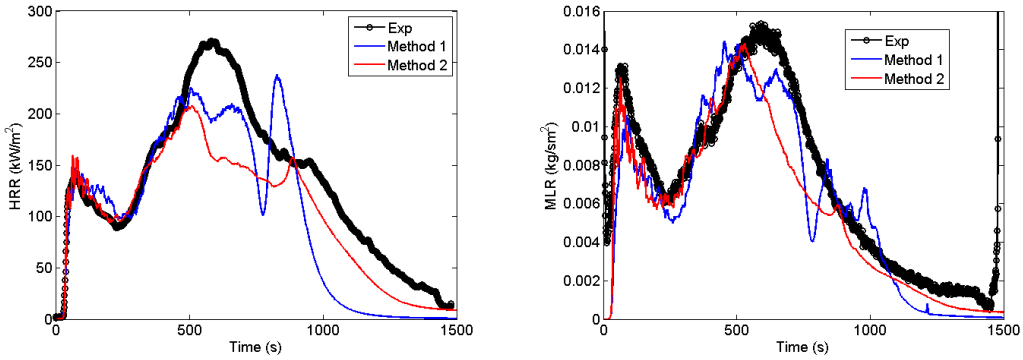

a) b)

Figure 12. Cone calorimeter results with oxidation at 50 kW/m2. a) Heat release rate. b) Mass loss rate.

Table 11. Parameters for surface oxidation of cable sheath.

	Method 1	Method 2
22.9 % of initial mass		
A (s^{-1})	$6.0 \cdot 10^{12}$	$2.5 \cdot 10^{10}$
E (kJ/kmol)	$2.5 \cdot 10^{5}$	$2.3 \cdot 10^{5}$
N	1.4	1.0
n_{O2}	1.5	1.5
y_F	0.34	0.34
k (W/m·K)	1.0	0.2
c_p (kJ/kg·K)	1.0	2.5
ΔH (kJ/kg)	0	1500
ash		
k (W/m·K)	0.122	0.6
c_p (kJ/kg·K)	3.5	3.0
ε	0.85	1.0

CONCLUSIONS

Unknown composition of the sample material is often a challenge in the pyrolysis and fire modelling. Since it is not practical to perform a complete chemical analysis of each material, alternative methods have been searched. An experimental tool, MCC, has been exploited for measuring the heat of combustion of each reaction and estimation of the sample composition.

Two new methods for combining MCC and TGA results were developed. First one is a simple and practical engineering solution that just measures the net heat release of each reaction. This approach is usually enough in order to make an accurate pyrolysis model. The second one has more ambitious goal to understanding better the sample material. It requires some knowledge about the chemical components and the degradation path of the material. This method may be more useful in the academic research projects than in engineering applications. Both methods were applied to two generic materials with known reaction paths and parameters, and to one real PVC mixture of an electric cable.

Both methods were verified to calculate the heat release of each reaction correctly. The method 2 was also validated by comparing the estimated and target values of the mass fractions, fuel yields and the heat of combustions of the reactions. The differences were very small considering that the parameters are known to compensate each other.

The methods 1 and 2 were finally used in the pyrolysis modelling of a real PVC cable. The results are realistic and predicting the small scale experiments accurately. The models were applied also in the bench scale using cone calorimeter results. The surface oxidation of char was also modelled. Surface oxidation is a significant phenomenon in the end of the cone calorimeter experiment and can be observed visually by the glowing surface. However, in the model this did not seem to make great difference because of the definition of the reaction paths.

Acknowledgements

The authors would like to thank Dr. Kevin McGrattan from NIST for the MCC and cone calorimeter results for cable #701 and Dr. Tuula Leskelä (Aalto University School of Science and Technology) for the TGA results. The work has been partially funded by the Nuclear Waste Management Fund of Finland (VYR).

References

1. Matala, A. and Hostikka, S. Pyrolysis Modelling of PVC Cable Materials. *Fire Safety Science -- Proceedings of the Tenth International Symposium*, International Association for Fire Safety Science, 2011, p. 917-930. DOI: 10.3801/IAFSS.FSS.10-917

2. Matala, A., Hostikka, S., Mangs, J. Estimation of Pyrolysis Model Parameters for Solid Materials Using Thermogravimetric Data. *Fire Safety Science -- Proceedings of the Ninth International Symposium*, International Association for Fire Safety Science, 2008, p. 1213-1224. DOI:10.3801/IAFSS.FSS.9-1213

3. Lautenberger, C., Rein, G., Fernandez-Pello, C. The application of a genetic algorithm to estimate material properties for fire modeling from bench-scale fire test data. Fire Safety Journal 41 (2006) 204-214. doi:10.1016/j.firesaf.2005.12.004

4. Lyon, R.E., Walters, R.N. Pyrolysis combustion flow calorimetry. Journal of analytical applied pyrolysis 71 (2004) 27-46 dx.doi.org/10.1016/S0165-2370(03)00096-2

5. Lyon, R.E., Walters, R.N., Stoliaroc, S.I., Safronava, N. Principles and Practise of Microscale Combustion Calorimetry. Federal Aviation Administration report DOT/FAA/TC-12/53, Springfield, Virginia, 2013. 89 p.

6. D. Drysdale. An Introduction to Fire Dynamics. 3rd edition. John Wiley and Sons, Ltd, UK., 2011.

7. Reaction-to-fire tests - heat release, smoke production and mass loss rate. ISO 5660-1, 2002.

8. NIST Special Publication 1019. Fire Dynamics Simulator. User's Guide. (2012)

9. McGrattan, K., Lock, A., Marsh, N., Nyden, M., Morgan, A.B., Galaska, M., Schenck, K. Cable Heat Release, Ignition, and Spread in Tray Installations During Fire (CHRISTIFIRE). Phase 1: Horizontal Trays. NUREG/CR-7010, Vol. 1. (2012)

10. Lattimer, R.P., Kroenke, W.J. The Formation of Volatile Pyrolyzates from Poly(vinyl Chloride). Journal of Applied Polymer Science, Vol. 25, 101-110 (1980)

11. Mountado, G., Puglisi, C. Evolution of Aromatics in the Thermal Degradation of Poly(vinyl chloride): A Mechanistic Study. Polymer Degradation and Stability 33 (1991) 229-262

12. Marcilla, A., Beltrán, M. PVC-plasticizer interactions during the thermal decomposition of PVC plastisols. Influence of the type of plastizicer and resin. Polymer Degradation and Stability 53 (1996) 261-268.

13. Jiménez, A., López, J., Vilaplana, J., Dussel, H.-J. Thermal degradation of plastisols. Effect of some additives on the evolution of gaseous products. Journal of Analytical and Applied Pyrolysis 40-41 (1997) 201-215.

14. Elakesh, E.O., Hull, T.R., Price, D., Milnes, G.J. Carty, P. Effect of Plasticizers on the Thermal Decomposition of Chlorinated Polyvinylchloride. Journal of Vinyl & Additive Technology (2005).

15. Marcilla, A., Beltrán, M. Effect of the plasticizer concentration and heating rate on the thermal decomposition behavior of PVC plastisols. Kinetic analysis. Polymer degradation and Stability 60 (1998) 1-10.

16. Miranda, R., Yang, J., Roy, C., Vasile, C. Vacuum pyrolysis of PVC I. Kinetic study. Polymer Degradation and Stability 64 (1999) 127-144.

17. Marcilla, A., Beltrán, M. Thermogravimetric kinetic study of poly(vinyl chloride) pyrolysis. Polymer Degradation and Stability 48 (1995) 219-229.

18. Marcilla, A., Beltrán, M. Kinetic models for the thermal decomposition of commercial PVC resins and plasticizers studied by thermogravimetric analysis. Polymer Degradation and Stability 53 (1996) 251-260.

19. Beltrán, M., Marcilla, A. Kinetic models for the thermal decomposition of PVC plastisols. Polymer Degradation and Stability 55 (1997) 73-87.

20. Kim, S. Pyrolysis kinetics of waste PVC pipe. Waste Management 21 (2001) 609-616.

21. Matala, A., Hostikka, S. Pyrolysis Modelling of PVC Cable Materials. Fire Safety Science 10 (2011).

22. Wypych, G. PVC Formulary. ChemTec Publishing. (2009) pp. 379.

23. Marcilla, A., Ruiz-Femenia, R., Hernández, J., García-Quesada, J.C. Thermal and catalytic pyrolysis of crosslinked polyethylene. Journal of Analytical Applied Pyrolysis 76 (2006) 254-259. doi:10.1016/j.jaap.2005.12.004